Dynamics and stability of anomalous Saffman-Taylor fingers

M. Rabaud, Y. Couder, and N. Gerard
Groupe de Physique des Solides de l'Ecole Normale Supérieure, 24 rue Lhomond, 75231 Paris Cédex 05, France
(Received 4 June 1987)

The existence of anomalous Saffman-Taylor fingers when a localized disturbance is applied at their tip has been demonstrated by several recent experiments. We show that they form a well-defined family with strong similarities with crystalline dendrites. They are narrower and more stable than normal fingers, their tip is parabolic, and its radius of curvature ρ is proportional to the capillary length l_0. For very large velocities, saturation occurs when ρ becomes of the order of the plate spacing. Using localized disturbance and periodic forcing we characterize the amplification of waves on their lateral fronts and we then discuss some implications for dendritic crystalline growth.

I. INTRODUCTION

Anomalous fingers form a new family of solutions in the classical Saffman-Taylor problem. In order to make clear the specificity of anomalous fingers we must recall the main characteristics of normal fingers. Since the early work of Saffman and Taylor,[1] these have been studied by many authors experimentally, numerically, and theoretically. Recent reviews about usual fingers can be found in Saffman,[2] Homsy,[3] and Bensimon *et al.*[4]

The motion of a fluid between two horizontal narrowly spaced solid plates is usually described by the two-dimensional velocity field averaged through the thickness of the cell. It is a potential field given by the Darcy law,

$$V=-\frac{b^2}{12\mu}\nabla p \ , \tag{1}$$

where μ is the dynamical viscosity of the fluid and b the spacing of the plates. If the fluid is incompressible the pressure satisfies Laplace's law $\Delta p=0$.

If two fluids of very different viscosities move together in a Hele-Shaw cell, their interface is unstable when the less viscous fluid forces the other to recede. When surface tension is negligible, all the wavelengths are unstable. The stability analysis of a moving plane front in the presence of interfacial tension T was done by Chuoke *et al.*[5] They consider a spatially periodic disturbance of wave vector k along the front and study its rate of amplification ω. In the case where a fluid of negligible viscosity (e.g., a gas) moves into a viscous fluid (e.g., oil), the dispersion relation can be written

$$\omega=V\,|\,k\,|\,\left[1-\frac{b^2}{12N_{\rm ca}}k^2\right] , \tag{2}$$

where $N_{\rm ca}=\mu V/T$ is the capillary number. The first destabilization of the interface occurs at a wavelength of the order of $l_c=2\pi/k_c$, where k_c is the wave vector of largest amplification rate given by (2),

$$k_c=2\frac{\sqrt{N_{\rm ca}}}{b}=\frac{1}{\sqrt{3}l_0} \ ,$$

where l_0 is the capillary-length scale of the problem traditionally chosen to be

$$l_0=\frac{b}{\sqrt{12N_{\rm ca}}} \ . \tag{3}$$

Experiments on this instability are concerned not only with its onset but also with its nonlinear growth. As the pressure is a Laplacian field, the choice of the boundary conditions in the plane of the cell is determinant for growth of the instability at large amplitudes. Saffman and Taylor[1] in their original experiment used a long channel of width W with closed lateral walls. We will refer to this as the linear geometry. More recently, Bataille[6] introduced an axisymmetric geometry where the air is injected at the center of a cell formed by two circular plates with opened boundary conditions at the periphery. We will refer to it as the circular geometry.

In the linear geometry the fastest initial finger screens off the others and forms a steady solution characterized by the fraction λ of the cell's width that it occupies and by its velocity U. (We will use this value of U thereafter in the definition of $N_{\rm ca}$ and l_0.)

The experiments[1,7,8] confirmed by numerical simulations[9–11] show that, increasing the capillary number, the finger tends towards $\lambda=0.5$. In other terms, the steady solution remains in a large range of velocities scaled uniquely on the width of the channel. However, with increasing velocities the ratio W/l_0 increases, so that, on the scale of the capillary length l_0, the forward front of the finger becomes nearly similar to a flat interface. It is surprising that this front has a large range of stability. A new parameter has been introduced,[10,11]

$$\frac{1}{B}=12\left[\frac{W}{b}\right]^2\frac{\mu U}{T}=12\left[\frac{W}{b}\right]^2 N_{\rm ca}=\left[\frac{W}{l_0}\right]^2 . \tag{4}$$

Its value measures how "far" the width scale W is from the capillary length scale $l_0(U)$. It is the only parameter

which enters in the selection of the finger width in an ideal two-dimensional situation.[8]

In the absence of surface tension, Saffman and Taylor[1] found a family of analytical solutions of the shape of the interface given by the equation

$$x=\frac{W(1-\lambda)}{2\pi}\ln\left[\frac{1}{2}\left[1+\cos\frac{2\pi y}{\lambda W}\right]\right]. \quad (5)$$

The curve obtained from Eq. (5) for $\lambda=0.5$ fits the observed finger shape but the selection of the finger has to be sought in the effect of surface tension.[9] This was done by Vanden-Broeck,[12] using numerical techniques, and by Combescot *et al.*,[13] Shraiman,[14] and Hong and Langer,[15] by analytical methods. They showed that only a discrete set of solutions satisfies the continuity of the derivative at the tip of the finger (solvability condition). In this set, $\lambda>0.5$, and it tends towards $\lambda=0.5$ when N_{ca} goes to infinity. The stability of these solutions was investigated by Kessler and Levine,[16] Bensimon,[17] and recently by Tanveer.[18]

We reported in a previous paper[19] the first observation of very different fingers. We showed that a local disturbance of the tip (we had used either a small bubble or a thread[20] stretched along the cell) led to fingers with relative widths λ much smaller than 0.5. Our interpretation was that by disturbing the tip we relax the solvability condition there, so that the selection of the discrete set of solutions is removed. The continuum of solutions given by Eq. (5) becomes possible. Indeed, the narrow fingers (that hereinafter we will call anomalous fingers) have the shape predicted by Eq. (5) for small λ. We also showed that the anomalous fingers obtained at a given value of the capillary number in various cells were selected for their dimensionless radius of curvature at the tip ρ/b. In other terms, the fingertip shape is determined by its velocity and it is only further along the profile that the finger "feels" the boundary conditions imposed by the lateral walls. There is, for anomalous fingers, a unique relation between ρ/b and N_{ca} in all cells. However, this relation remained incompletely investigated; in particular, the saturation of ρ/b at larger N_{ca} was not fully understood.

Simultaneously Kessler *et al.*[21] found that when the surface tension was taken to be anisotropic a new family of fingers was obtained where λ decreased continuously with increasing capillary number. A similar result has been obtained by Dorsey and Martin.[22]

More recently, Hong and Langer[23] have shown that if a finite angle was assumed at the tip, narrow fingers of the type we had observed were selected. Zocchi *et al.*[24] have investigated the anomalous fingers obtained with a thread and shown that the effect of the thread could be simulated in a two-dimensional model by a local weakening of the surface tension.

These various works strongly suggest that narrow fingers form, as we had suggested, a new family of solutions with well-determined properties. They appear with a large variety of disturbances at the tip, as is shown also by experiments in the circular configuration.[25–29]

In the present article, which is the continuation of Couder *et al.*,[19] we address ourselves to three problems.

In otherwise similar experimental conditions we check that three different types of tip disturbances give rise to the same family of anomalous fingers (Sec. III A).

We establish the precise relation ρ/b versus N_{ca} and give an interpretation of the observed saturation (Sec. III B).

In order to investigate the stability of anomalous fingers, we study the impulsional response of their fronts to a localized disturbance as well as the effect of a periodic forcing (Sec. III D).

In Sec. IV we will discuss the strong similarities between the formation of anomalous fingers and the growth of crystalline dendrites.

II. EXPERIMENTAL SETUP

Most of the experimental cells were built with glass plates of thickness 1.5 cm and length 150 cm. Because it lends itself more easily to mechanical engraving, we also used a cell made with two Perspex plates of the same dimensions. The flexion of the plates, however, limited the use of this particular cell to low applied pressure and thus to small velocities of the finger.

We investigated the anomalous fingers in cells of various dimensions. We define their aspect ratio as $\Gamma=W/b$, where W is the width of the channel and b its thickness. We used mainly cells with $\Gamma=120,60,40,20$ ($W=12$, 6, 4, and 2 cm and $b=0.1$ cm). A few experiments were also done in cells with $\Gamma=280$ ($W=28$ cm, $b=0.1$ cm), $\Gamma=240$ ($W=12$ cm, $b=0.05$ cm), and $\Gamma=120$ ($W=6$ cm, $b=0.05$ cm). In all the cells the two glass plates were clamped together with longitudinal spacers on both sides, forming the lateral walls of the channel. The width was defined to better than $\Delta W=0.05$ cm and the thickness to $\Delta b=0.005$ cm.

The cell was filled with silicon oil, Rhodorsil 47 V 100, which has a surface tension $T=20.9\times10^{-3}$ N/m at 25 °C and a viscosity $\mu=96.5\times10^{-3}$ kg/m s. The less viscous fluid was nitrogen gas and was injected into the cell at a tunable pressure.

We used three different techniques to disturb the tip of the fingers. As we will see, their effect in creating narrow fingers was similar but the stability of the resulting fingers was different.

In one series of experiments we had a thin groove engraved in the middle of each plate. The grooves had a triangular profile; their width was approximately 0.08 cm and their depth 0.04 cm. The plates were then mounted so that the two longitudinal grooves exactly faced each other along the axis of the cell.

In the second series of experiments, we stretched a thin and regular nylon thread (120 μm in diameter) from one end of the cell to the other. It could be set either along the axis or at a distance y_1 from it.

Finally, using a long hypodermic needle, we injected small air bubbles in the cell ahead of the moving front. When one of the growing initial fingers caught up with a bubble, it moved faster so that it overcame the others and established itself in the center of the cell.

The shape of the resulting fingers was analyzed on

photographs. For systematic measurements videotape recordings of the experiments were used. The width of the finger was measured with a precision of 0.05 cm. The accuracy of the velocity measurements was limited by the frame repetition rate and was of the order of $\Delta v/v \approx 10^{-2}$.

In order to study the stability of the fingers, we disturbed them either by localized perturbations or by periodic modulation of the velocity. The use of a thread lent itself easily to the introduction of a localized disturbance (such as by having a knot on it). We have also applied a periodic forcing of the finger by modulating the applied pressure. The input of nitrogen gas had a buffer volume V_0 connected with a cylinder of volume $V_1 \approx 10$ cm^3 in which a piston was moved by a motor at regulated frequency f. The amplitude of the resulting pressure modulation could be chosen by changing the volume of the buffer. The applied pressure was given by a pressure gauge and recorded as a function of time in order to obtain a measurement of the mean pressure, of the rate of modulation, and to check that no harmonic frequency had been created. The resulting modulation of the velocity and destabilization of the finger were observed on videotape recordings.

III. EXPERIMENTAL RESULTS

A. Finger tips and finger shapes

As we will see, the overall shape of anomalous fingers depends only weakly on which type of disturbance has been applied at the tip of the finger. This is rather surprising, as the distortion of the tip itself looks very different in the three cases. In the present section we are going to describe the distortion of the tip in each case and its effect on the general shape of the finger.

1. The perturbation by two grooves or a thread

The effect of the two opposite grooves is the simplest. The tip of the finger remains localized between the grooves and the distortion created by them is small. We showed previously[19] that the shape of the anomalous fingers is very well fitted by the analytical solutions of Saffman and Taylor in the absence of surface tension given by Eq. (5). This is particularly true for the fingers obtained with grooves. They only depart from the theoretical profile in the region of the tip which is very slightly sharper [Figs. 1(a) and 2(a)].

The presence of a thread [Fig. 1(b)] has a more complicated effect. Careful observation shows that the thread does not actually cross the oil-air interface. It remains coated with an oil film which is linked by a meniscus to the oil film left on one of the glass plates. The thread is therefore at the top of a longitudinal oil meniscus which forms a linear ridge inside the air finger. The in-plane profile shows a flat part above the thread. As a result the tip forms itself in either of two symmetrical positions at a distance Δy from the thread. Experimentally, Δy varies as $U^{-1/2}$ so that, in a large range of velocities, as the profile is nearly parabolic, the angle θ_0 of the thread with the normal to the finger remains constant. We found θ_0 of the order of 45°. If the thread is at the center of the cell, the resulting fingers are slightly asymmetrical. But the thread can be placed off center at a distance y_1 from the axis. The tip is then at a distance $y_0 = y_1 \pm \Delta y$ from the center line. It is possible to obtain symmetrical fingers when $y_1 - \Delta y = 0$ (this correction,

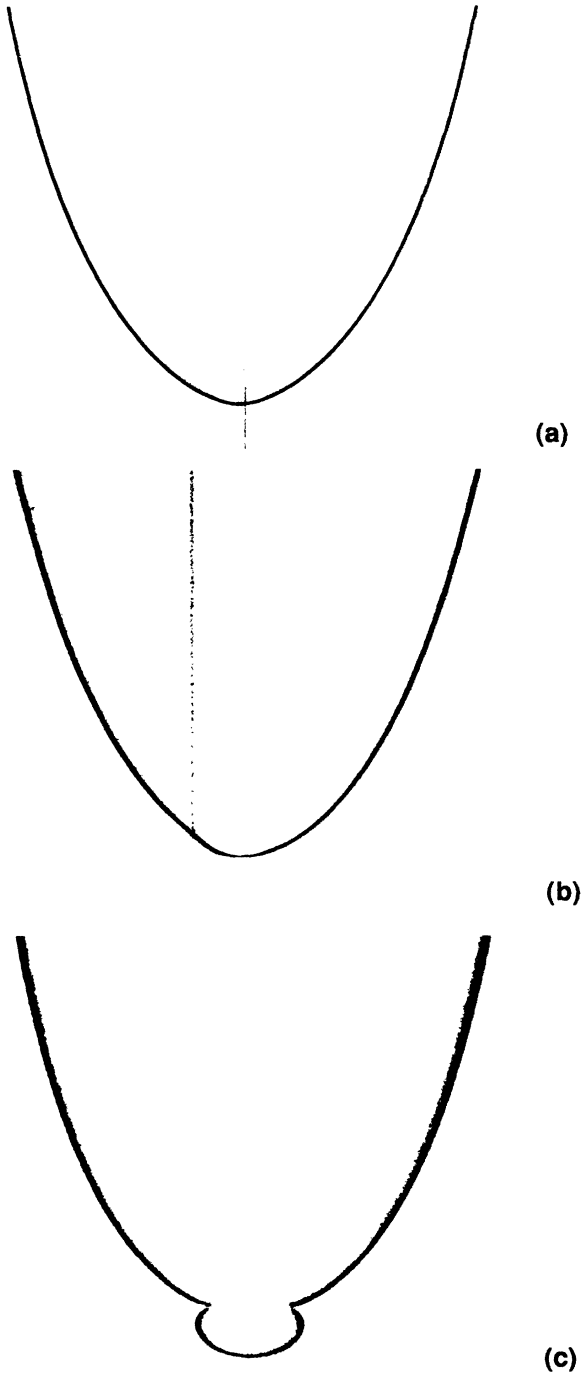

FIG. 1. Photographs of the finger tip with the three different types of perturbation. (a) Two opposite grooves etched in the plates. (b) A thin thread stretched along the cell. (c) A small bubble.

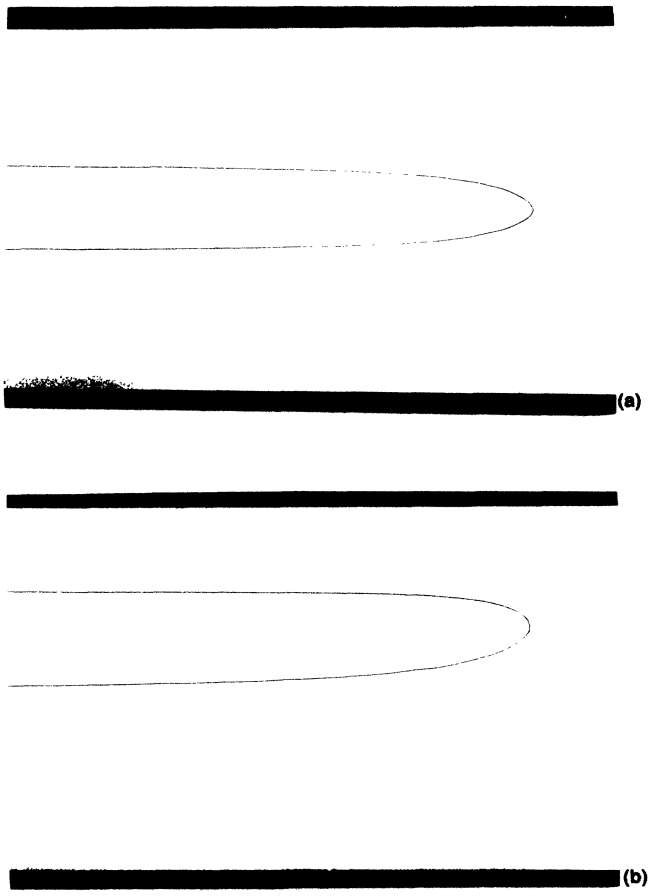

FIG. 2. Two stable narrow fingers. (a) A finger $\lambda=0.22$ obtained in a cell $W=12$ cm and $b=0.1$ cm, with two grooves. (b) An asymmetrical finger obtained with a laterally displaced thread. $y_1=2$ cm, $\Delta y=0.2$ cm, $y_0=2.2$ cm, and $\lambda=0.26$, in a cell $W=12$ cm and $b=0.1$ cm.

however, is not perfect at all velocities, as Δy is a function of U). When the thread is purposefully placed far from the axis, very asymmetrical fingers can be obtained [Fig. 2(b)]. Their shape is well fitted by analytical solutions also found by Taylor and Saffman[30] and given by the equation

$$x=\frac{W(1-\lambda)}{\pi}\ln\left[\cos\frac{\pi}{\lambda}\left[\frac{y-y_0}{W}\right]\right]+\frac{2y_0}{\pi}\ln\left[\tan\frac{\pi}{4}\left[1+\frac{2(y-y_0)}{W\lambda}\right]\right], \quad (6)$$

where y_0 (transverse distance of the tip to the axis of the cell) and λ (relative width of the finger) are the two independent parameters. These solutions were not observed in undisturbed cells.

The effect of the grooves or the thread is due to the breaking of the homogeneity of the cell as the thickness is either increased or decreased along a line. The classical treatment of the Saffman-Taylor instability, in order to reduce the problem to a two-dimensional one, requires the spatial homogeneity of the cell for two reasons. It is necessary to establish Eq. (1), where b must be constant, and it is also necessary to model the capillary effects. The meniscus between the two fluids has two curvatures. The strongest is the transverse curvature between the glass plates, usually assumed to be constant and equal to $2/b$. The variations of the Laplace pressure along the profile are then considered to be due only to the changes of the in-plane two-dimensional curvature.

Two grooves engraved in the glass plates create a local increase of the cell thickness. As a result the transverse curvature of the meniscus is decreased between the grooves. An equilibrium of the Laplace pressure in the vicinity of the grooves is then reached as the in-plane curvature becomes larger. This zone of larger curvature will move faster by point effect and will be stable at the tip of the finger. The introduction of a three-dimensional disturbance has created a singular region in the two-dimensional problem.

When a thread is used, the increase of the normal curvature will result in a local decrease of the in-plane curvature which corresponds to the observed flat [Fig. 1(b)]. The modeling of the effect of these disturbances can be achieved in two dimensions by assuming a local variation of the surface tension. Recently, Zocchi *et al.*[24] have studied numerically a model where, along an interface line, they assume a local weakening of surface tension. They obtain anomalous fingers and the disturbed zone stabilizes either at the tip or on the side of the finger, two situations which are in agreement with those observed, respectively, with two grooves or a thread.

2. *The perturbation with a small bubble*

The introduction of a small bubble is a different way of locally getting around the strict laws of the Hele-Shaw cell. While the grooves or the thread created local three dimensionality, the bubble is a topological expedient. The main point is that the bubble is closed on itself and its radius of curvature can be much smaller than the length scale l_0. It can thus create artificially a sharper point to the finger [Fig. 1(c)]. To obtain a stable situation the bubble has to be pressed against the finger tip so that it creates a small depression at its extremity. For very small velocities this is not realized, so that the bubble is advected away along one of the finger sides. For this reason anomalous fingers created by a bubble are observed in a smaller range of velocities than with the other techniques.[19] The anomalous fingers have the same shape as those obtained with the grooves, except in the tip region, where the bubble protrudes in front of the profile.

B. Finger selection

In the laboratory experiments the actual control parameter is the applied air pressure which can be tuned at will. As observed previously,[19] for a given pressure, anomalous fingers grow faster than normal ones (because they are sharper). However, the various types of disturbance are not of the same efficiency so that fingers disturbed differently will not necessarily have the same ve-

locity for the same applied pressure.

This would appear to make the study of anomalous fingers difficult. In fact, we will not study here how the velocity results from both the applied pressure and the type of the disturbance. But we show that the same fingers are observed at the same velocity with a bubble, a thread, or two grooves (except in the distorted region at the tip). These fingers form a well-defined family of solutions that we study by recording their shape as a function of velocity in cells of different aspect ratio.

We showed[19] that the shapes of the anomalous fingers are well fitted by solutions of Eq. (5). This is, of course, only true in the regimes where the capillary number is large enough. In our case, the fit is excellent in all cases with $\lambda < 0.5$. The experimental profiles only depart from the theoretical ones in the disturbed region (in particular, the bubble protrudes in front of the profiles).

We had also shown that at a given velocity the anomalous fingers obtained in cells of different aspect ratios have different widths but the same adimensional radius of curvature ρ/b at their tip (Fig. 3 of Ref. 19). Experiment shows that, dynamically, it is this region which selects the finger shapes. In order to have a good precision we do not measure ρ directly. We deduce it from the observed λ. In the profiles defined by Eq. (5), the parabolic approximation gives

$$\rho = \frac{\lambda^2 W}{\pi(1-\lambda)} . \tag{7}$$

It might seem paradoxical to choose a characteristic of the disturbed region to define the finger shape. This can be justified by Fig. 3, where we superimpose three finger shapes that would be obtained at the same velocity in three cells of different width, but same thickness. In the narrowest cell, of width W_1, we chose a solution of Eq. (5) corresponding to $\lambda = 0.23$. In a cell with $W = 2W_1$, the finger with the same curvature will have a width $\lambda = 0.165$. As W increases, λ decreases, and the region in which the finger is nearly parabolic grows. The third finger in Fig. 3 is the limiting parabola that would be obtained for an infinite width ($\lambda \to 0$ for $W \to \infty$). Throughout this article we will be concerned with anomalous fingers in wide cells; as they correspond to small values of λ, their extremity is parabolic in a zone which is much larger than the region disturbed by the grooves, the thread, or the bubble. The parabolic approximation is then justified.

We can now complete our previous work by discussing the evolution of ρ/b with N_{ca} and its saturation at large velocities. Our present results are consistent with those presented in Ref. 19 but more precise for two reasons. The use of the grooves or the thread rather than the bubble creates anomalous fingers that are stable at low velocities, and we also have cells of larger aspect ratio, so fingers of small λ are observed in larger range of values of N_{ca}.

Figure 4 shows the plot of the dimensionless radius of curvature ρ/b as a function of the dimensionless capillary length $l_0/b = (12N_{ca})^{-1/2}$. The experimental points were obtained in a cell $W = 12$ cm and $b = 0.1$ cm disturbed by a thread. Two regimes are clearly observed.

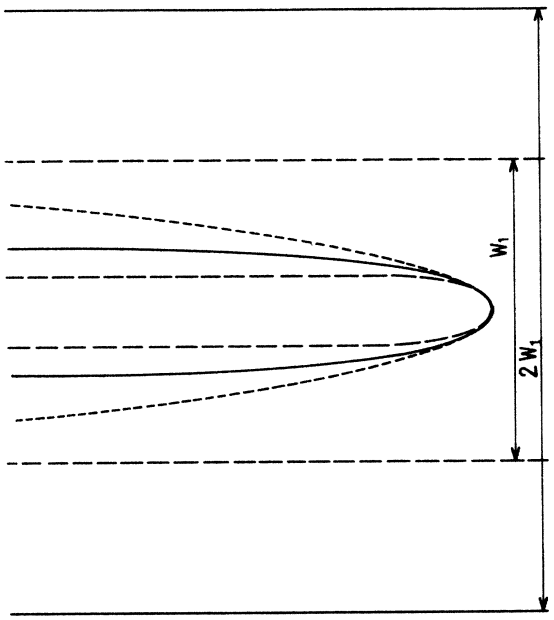

FIG. 3. Three superimposed solutions of Eq. (5) which have been scaled to have the same radius of curvature at the tip. They correspond to the fingers that will be physically obtained at the same velocity in cells of same thickness but different width. — — —, $W = W_1$, $\lambda = 0.23$; ——, $W = 2W_1$, $\lambda = 0.165$; ---, $W \to \infty$, $\lambda \to 0$.

In a large range of velocities, ρ is proportional to l_0,

$$\rho = \alpha l_0 \quad (\text{with } \alpha = 4.1 \pm 0.1) .$$

At large velocities (small l_0/b), a crossover occurs to a regime where ρ/b remains constant at a value β,

$$\rho = \beta b \quad (\text{with } \beta = 2.2 \pm 0.1) .$$

Table I summarizes the results obtained in other cells with various disturbances. They are consistent with the previous description. However, the results obtained

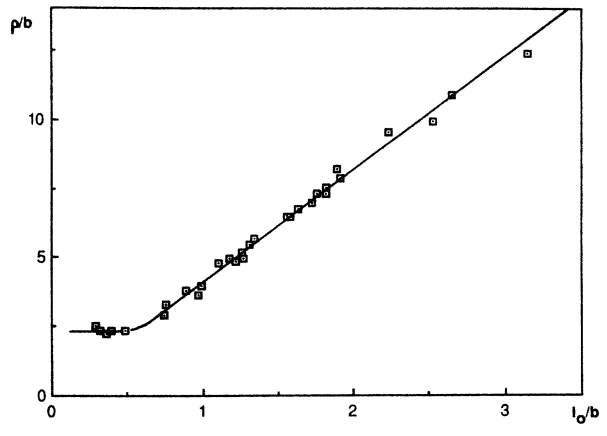

FIG. 4. Plot of the dimensionless radius of curvature at the tip, ρ/b as a function of the dimensionless capillary length $l_0/b = (12N_{ca})^{-1/2}$, in a cell $W = 12$ cm and $b = 0.1$ cm.

TABLE I. Values of α, β, and λ_{min} obtained in cells of different dimensions with various perturbations.

Perturbation	Geometry (cm)	α	β	λ_{min}
thread	$W=28$, $b=0.1$	4.0±0.1		
thread	$W=12$, $b=0.1$	4.1±0.1	2.2±0.1	0.22
thread	$W=4.7$, $b=0.1$	3.8±0.2	2.4±0.1	0.33
thread	$W=12$, $b=0.05$	4.0±0.2	3.0±1.0	0.18
thread	$W=12$, $b=0.2$	4.0±0.3	2.4±0.1	0.30
grooves	$W=12$, $b=0.1$	3.5±0.2	2±0.1	0.20
bubble	$W=12$, $b=0.2$	3.2±0.2	2.5±0.1	0.30
bubble	$W=12$, $b=0.1$	3.1±0.2	2.3±0.2	0.22
bubble	$W=6$, $b=0.1$	3.5±0.3	2.4±0.1	0.29
bubble	$W=4$, $b=0.1$	3.3±0.3	2.5±0.1	0.35

with cells of small aspect ratio correspond to a less accurate proportionality between ρ and l_0. This can be understood, as it is only in cells of large aspect ratio that we can have simultaneously $\rho \gg b$ and $\rho \ll W$. The first condition must be met to avoid saturation, and the second to have narrow fingers with $\lambda < 0.5$ which are fitted by Eq. (5). The same behavior is observed in all cells with the three types of disturbance. It appears, however, that the values of α slightly depend on the disturbance. The value obtained with a thread is $\alpha \approx 4.0 \pm 0.2$, while it is $\alpha \approx 3.5 \pm 0.3$ for grooves or for a bubble. This discrepancy is probably due to the neglect of the asymmetry induced by the thread. The value of β is poorly measured in the cells of thickness 0.05 cm because, under strong applied pressure, flexions of the plates are no longer negligible. The spacing b widens and both ρ and λ tend to increase slightly with velocity.

The first regime where $\rho = \alpha l_0$ corresponds to a situation very different from normal fingers. Here the curvature ρ remains scaled on the unstable length scale of a front moving at U so that the product $\rho^2 U$ is constant in a given cell,

$$\rho^2 U = \frac{\alpha^2 b^2 T}{12\mu} = \text{const.}$$

As a result, the finger tip always remains stable. A law of this type links the radius of curvature and the velocity of parabolic crystalline dendrites.[31]

We interpret the second regime by noting that the value of β is small, so that the two curvatures of the meniscus are of the same order of magnitude. The saturation is due to the breaking of the two dimensionality. We must remember here that Eq. (1) is built on averaging through the cell thickness, which assumes that the in-plane scale of the flow is large compared to b. This is no longer true here. This result is consistent with a previous observation by Paterson[32] in an experiment using two miscible fluids in the circular geometry. In this zero-surface-tension limit, where the capillary length has vanished, he observed a dense structure of fingers with a finite width related to the cell thickness and of the order of $4b$.

The crossover between the two types of determinations of ρ occurs at fixed values of N_{ca} when $\alpha l_0 = \beta b$. As a result, in all cells for values of $N_{ca} \geq 0.18 \pm 0.02$, the thickness becomes dominant and λ saturates. We must underline, therefore, that the observed saturations of the values of λ of anomalous fingers are in no way comparable to the saturation of normal fingers at $\lambda = 0.5$.

Finally, for the sake of comparison with the classical results we can plot λ as a function of $1/B$. If such a plot reconciles all the results of classical fingers it does not for anomalous ones (Fig. 5). Before the saturation there is a common curve which can be obtained by solving

$$\rho = \alpha l_0 ,$$

where ρ and l_0 are given by Eqs. (7) and (3). This gives

$$\lambda = \frac{\pi\alpha\sqrt{B}}{2}\left[\left[1+\frac{4}{\pi\alpha\sqrt{B}}\right]^{1/2} - 1\right] . \tag{8}$$

In this diagram, the crossover to the saturation occurs at values of $(1/B)_c$ dependent upon W/b,

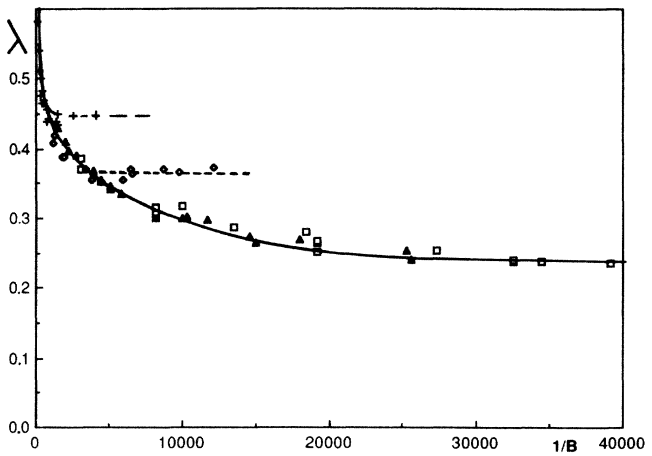

FIG. 5. Plot of the observed values of λ as a function of $1/B$ in four cells. ▲, $W=28$ cm, $b=0.1$ cm; □, $W=12$ cm, $b=0.1$ cm; ◇, $W=4$ cm, $b=0.1$ cm; +, $W=2$ cm, $b=0.1$ cm. (The saturations of λ in the two wider cells are not in the range of values of $1/B$ shown here.)

$$(1/B)_c=(\alpha/\beta)^2(W/b)^2 .$$

When ρ saturates at $\rho=\beta b$, so does λ at a minimum value (cf. Table I),

$$\lambda_{\min}=\frac{\pi\beta b}{2W}\left[\left[1+\frac{4W}{\pi\beta b}\right]^{1/2}-1\right] . \quad (9)$$

C. The destabilization of anomalous fingers

Stability of the normal fingers has been reported[7,8] to break down at a value of $1/B\approx 5000$. Anomalous fingers can be observed stable up to values of $1/B\approx 450\times 10^3$. The reason for this larger stability is that tip splitting, the most dangerous instability for viscous fingers, is here totally inhibited. In contrast to classical fingers, anomalous fingers have a continuous adaptation of ρ with the natural unstable wavelength $l_c=2\pi\sqrt{3}l_0$, so that they are more stable. At larger velocity their destabilization is characterized by the formation of lateral undulations.

In fact, the parameter $1/B$ does not have the same meaning for normal and anomalous fingers. Normal fingers where $\lambda\rightarrow 0.5$ with increasing N_{ca} have a radius of curvature at the tip which remains scaled on W, so that $1/B=(W/l_0)^2$ is proportional to the square of the number of unstable wavelength l_c in the forward front of the finger. For anomalous fingers the radius of curvature at the tip follows the evolution of l_0 (Fig. 3). It is only the extent of the parabolic region of the finger which is scaled on W. This parabolic region is the zone of amplification of secondary lateral perturbations that we are going to study.

The aspect of the destabilization of the anomalous fingers is very dependent on the type of disturbance which has been applied at the tip. We will describe separately the two types of spontaneous destabilization which are observed.

(i) Figure 6(a) shows the type of unstable fingers obtained with either the grooves or the thread. In both cases, when velocity is increased, small-amplitude waves appear on the sides of the finger. There is no clear onset to their appearance. These waves have a determined wavelength but no long-range phase correlation. They appear as a succession of uncorrelated wave packets with a mean wavelength l_n. There is no spatial phase correlation between the waves on the two sides of the finger. This natural destabilization must be generated by the noise in the tip region. In fact, we do observe that it occurs at lower values of N_{ca} when the glass plates are dirty, scratched, or when the thread has been voluntarily roughened by means of sand paper. In the case of the thread, the most unstable side of the finger is always the side through which the thread passes. In the range where instability occurs spontaneously, the mean lateral wavelength has a dependence on N_{ca} shown in Fig. 7. We find that l_n is proportional to ρ,

$$l_n\approx(5.6\pm 0.4)\rho .$$

Fingers in cells of large aspect ratio become unstable at a smaller value of N_{ca} because the parabolic zone in

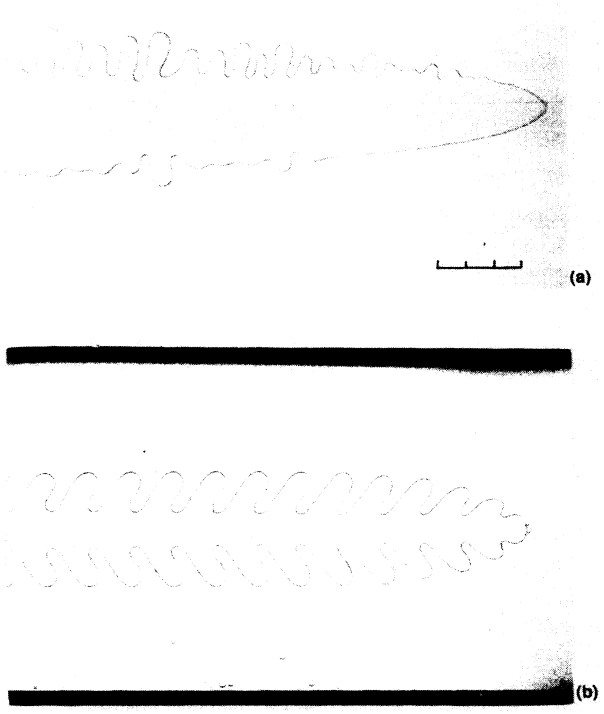

FIG. 6. (a) Spontaneous destabilization of anomalous fingers in a cell of width $W=28$ cm and $b=0.1$ cm disturbed by a thread. As the finger is very narrow ($\lambda=0.18$), only the central region of the cell is shown on this photograph and the lateral walls are far on each side. The scale is in centimeters. (b) A resonant mode obtained with a bubble in a cell $W=12$ cm and $b=0.1$ cm. The outer envelope of this oscillating symmetrical mode corresponds to a solution of Eq. (5) for $\lambda'=0.36$.

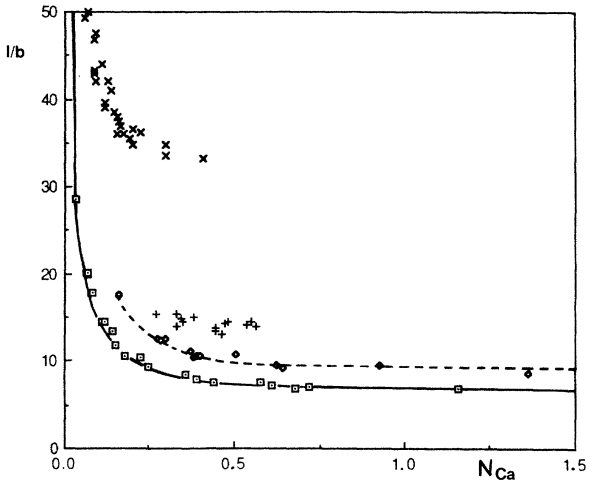

FIG. 7. Dimensionless wavelengths l/b observed on the side of an anomalous finger as a function of its dimensionless velocity N_{ca} ($W=12$ cm, $b=0.1$ cm). □ and ——, l_k generated by a knot; ◇ and — — —, l_n generated by lower amplitude disturbances; +, resonant mode l_s obtained with a bubble; ×, resonant mode l_{as} obtained with a bubble.

which the disturbance is amplified is larger.

(ii) When a bubble is used at the tip, the destabilization is very different. For a given bubble, it occurs at a clear onset value of N_{ca} and then sustains itself with a well-defined amplitude. Furthermore, the wave on each side is strictly periodic with a sharply defined wavelength and constant amplitude. Two modes of different wavelength, l_s or l_{as}, can be observed.[17,28] The shorter wavelength mode l_s is symmetric, the tip pulses with periodic changes of curvature and generates waves in phase on both sides of the finger [Fig. 6(b)]. The longer wavelength mode l_{as} is antisymmetric, the tip oscillates transversally and generates waves of opposite phase on each side of the finger [Fig. 5(b) or Ref. 19]. In both these cases the tip region seems to have localized resonant modes with the bubble, so that large amplitude modulation of the tip shape occurs with temporal frequency $U/1_s$ or U/l_{as}. The experiments show that the velocity at which the finger destabilizes depends on the bubble size. Large bubbles have smaller resonant frequencies, so that the finger destabilizes at low velocities in the antisymmetric mode (Fig. 7). With small bubbles it destabilizes at larger velocities in the symmetric mode (Fig. 7). In both cases, l_s and l_{as} are larger than l_n. In cells of large aspect ratio the wave can reach such a large amplitude that it begins to look like the side branching which is observed in the circular geometry.[28] It is worth noting that the outer envelopes of the waves are well fitted by solutions of Eq. (5). In Fig. 6(b) the destabilization of the finger with $\lambda=0.23$ led to a finger with side branching which has an envelope corresponding to $\lambda'=0.36$.

D. Response of the anomalous fingers front to external disturbances

We now return to the case of fingers generated with two grooves or a thread. In order to study the processes of selection of the unstable wavelength as well as the growth of the wave along the finger profile, we have chosen not to rely on the natural destabilization but to perturb the translating finger. We used two types of disturbances aimed at obtaining information on the stability of the profile. We either created a strong localized perturbation or we applied periodic forcing to the finger.

1. Impulsional response

In the case where a thread is used, it is easy to create a local disturbance by introducing a knot on the thread. When the meniscus touches the knot, it remains blocked on it for a short while. When it is released and starts moving again, a local narrow dip is created on one side of the finger profile. Figures 8 and 9 show the temporal evolution of this disturbance drawn from successive images of a videotape recording. For clarity, these pictures are shown as they appear in the laboratory (Fig. 8) and in the finger (Fig. 9) frames of reference. The following characteristics are observed.

The initial localized dip gives rise, in time, to a spreading wave packet with a growing spatial extent. As

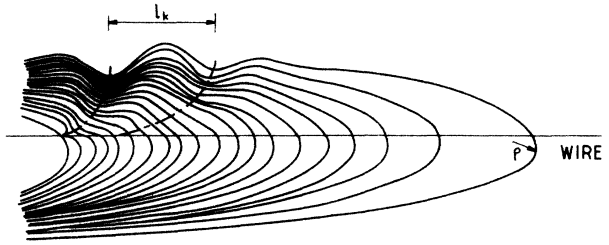

FIG. 8. Growth of a disturbance due to a knot on the thread as observed in the laboratory frame (drawings transferred from a tape recording). Except for the last two profiles, the images are taken 0.2 s apart.

the initial disturbance is advected away from the tip, new wavelets of decreasing amplitude appear near the tip. This shows that the waves are dispersed and have a nonzero group velocity in the laboratory frame. Figure 8 shows the further growth of each wavelet as it is advected along the profile.

The phase velocity of the wave can be directly observed. A given maximum of the wave is not motionless in the laboratory frame; its trajectory is shown in Fig. 8. The distance between two successive maxima grows as the waves are advected along the finger. This is, to our knowledge, the first direct experimental visualization of

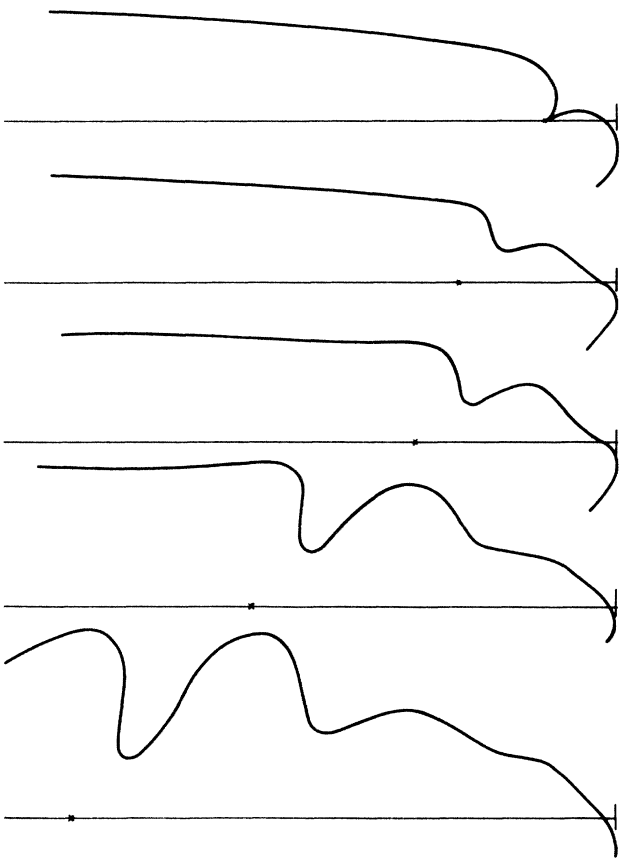

FIG. 9. Similar effect as observed in the finger frame of reference. The successive profiles correspond to the instants $t_0=0$ s, $t_1=0.06$ s, $t_2=0.10$ s, $t_3=0.22$ s, and $t_4=0.38$ s.

a wavelength stretching along a curved interface. A phenomenon of this type was first introduced theoretically by Zel'dovich *et al.*[33] in their discussion of the stability of flame fronts. Pelcé *et al.*[34] have shown that the same stretching was to be expected in the Saffman-Taylor fingers (as well as in the dendrites) and had to be taken into account in their stability. They consider that the motion of each maximum of the wave is similar to that of the fluid particle of the interface. As the anomalous fingers are fitted by the solution of Eq. (5), surface tension can be neglected everywhere but at the tip. In this limit the interface is an isobar and a fluid particle has in the laboratory frame a normal velocity

$$U_n = U\cos\theta \begin{cases} u_x = U\cos^2\theta \\ u_y = U\cos\theta\sin\theta \end{cases},$$

where θ is the local angle of the normal to the interface with the axis $0x$ of the cell.

Experimentally, the wave has this phase velocity and becomes motionless in the laboratory frame far from the tip, where $\theta \to \pi/2$. The corresponding velocity in the finger frame of reference is tangential to the profile,

$$U_t' = -U\sin\theta \begin{cases} u_x' = -U\sin^2\theta \\ u_y' = +U\sin\theta\cos\theta \end{cases}.$$

The advection along a curved profile creates a spatial variation of the wavelength l, given by

$$\frac{1}{l}\frac{dl}{ds} = \frac{1}{\sin\theta}\frac{d(\sin\theta)}{ds},$$

where s is the curvilinear abscissa. This equation can be integrated between the knot (where $\theta_0 \approx 45°$) and the side of the finger (where $\theta_1 = 90°$), and gives

$$l(\theta_1) = l(\theta_0)\frac{\sin\theta_1}{\sin\theta_0} = \sqrt{2}\, l(\theta_0).$$

The stretching actually observed in our experiments can be measured on the successive profiles of Fig. 8. Between the thread and the lateral side of the finger, the observed wavelength is stretched by a factor of the order of 2.5. This value is larger than that which would be simply due to the kinematic effect described above.[35] But here a wave packet has been generated initially, it contains components of all frequencies. Caroli *et al.*[36] have calculated the apparent stretching which results from the shift of the wavelength of maximum amplification when the wave packet is advected along the curved finger profile. A contribution of this type probably adds up here to the Zel'dovich stretching effect. We must, however, underline that we are in experimental conditions which are far from the infinitesimal amplitudes considered in theories. In our case the amplitudes are large so that nonlinear effects also come in. Furthermore, it is usually assumed that the perturbation wavelengths are small compared to local radius of curvature, a condition which is hardly satisfied here.

Finally we measure l_k, the wavelength of the wave packets created by the knot, far on the side of the finger, as a function of the velocity of the finger (Fig. 7). For a given velocity, l_k is smaller than l_n, the wavelength of the natural destabilization due to noise. Because it results from a large amplitude impulse, the evolution of l_k forms in the l-(N_{ca}) diagram, the lower limit of the domain of possible waves excited by noise on the finger sides. The logarithmic plot of Fig. 10 shows that l_k is proportional to the radius of curvature at the tip ρ. At low velocities both ρ and l_k are proportional to l_0; at large velocities both saturate and become proportional to b. At all velocities we have

$$l_k \approx 4.2\rho .$$

2. *Periodic forcing*

Periodic forcing gives different information on the destabilization of the fingers because the Zel'dovich stretching and the wavelength selection are observed separately. We limit ourselves here to the results obtained with two grooves or a thread. As we impose sinusoidal variation of the applied pressure we modulate the finger velocity U at a tunable frequency. In the case of two grooves the waves obtained on both sides of the finger are symmetrical and of limited amplitude. In the case of a thread there is a strong asymmetry between the observed waves on both sides of the finger. The side through which the thread passes appears to be more unstable than the other one. The reason is probably that the thread is surrounded by a complicated meniscus which changes shape when velocity is modulated. It creates a finite amplitude disturbance, periodic in time, localized near the thread. Because this initial disturbance is localized, its growth demonstrates best the amplification process along the profile.

For frequencies larger than a limit f_m, no effect on the finger is observed. Just below this threshold a wave grows near the thread and is rapidly damped further on [Fig. 11(a)]. For lower frequencies the amplification increases [Fig. 11(b)]. The modulation has a maximum efficiency at a frequency f_c [Fig. 11(c)]. The observed

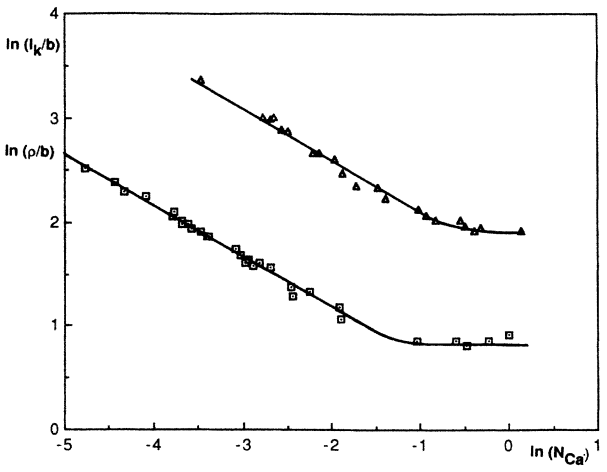

FIG. 10. Logarithmic plot of l_k (△) and ρ (⊡) as a function of the capillary number N_{ca} ($W = 12$ cm, $b = 0.1$ cm).

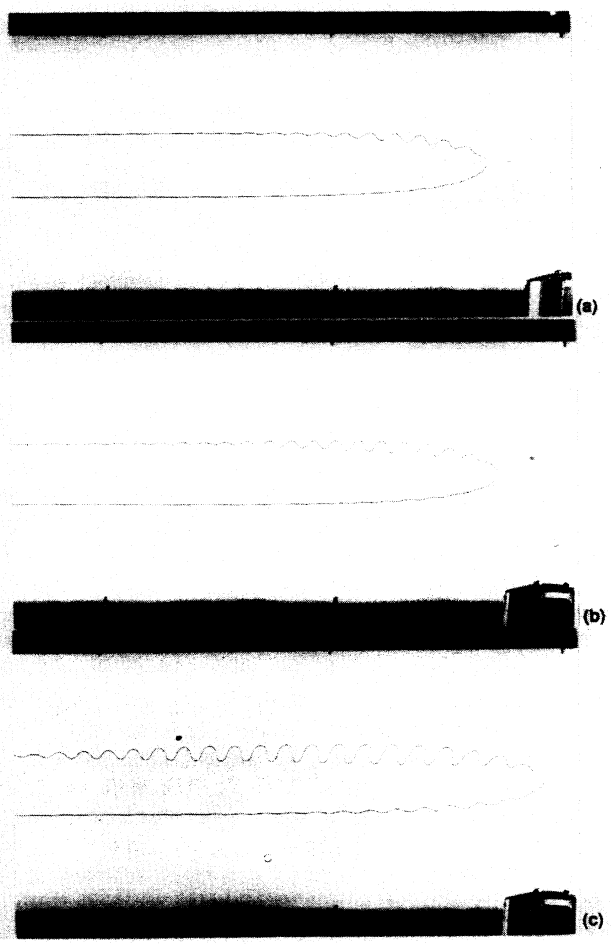

FIG. 11. Aspect of the wave generated on a finger (case of a thread) at different forcing frequencies ($W=12$ cm, $b=0.1$ cm). (a) $f\approx f_m$, (b) $f_c<f<f_m$, (c) $f\approx f_c$.

wavelength on the finger side is, in each case, $l=U/f$. The time periodic distortion of the meniscus around the thread creates at this point a deformation of the profile with, due to the tangential velocity, a spatial periodicity $l(\theta_0)=U\sin\theta_0/f$ [corresponding to a wave vector $k(\theta_0)=2\pi f/U\sin\theta_0$]. As this deformation is advected away, it undergoes kinematic stretching due to the variation of $\sin\theta$, so that along the linear side of the finger it will have a periodicity $l(\theta=\pi/2)=U/f$. We can obtain a qualitative description of the involved process in the following schematic description.

Let us recall that the stability of a plane interface translating at velocity U in a direction forming an angle θ with its normal is characterized by an equation of the type of (2),

$$\omega=U\mid k\mid\left[\cos\theta-\frac{b^2k^2}{12N_{\rm ca}\cos\theta}\right], \tag{10}$$

the range of unstable wave vectors is

$$0<k<k_m \quad \text{with } k_m=\frac{\sqrt{12N_{\rm ca}}}{b}\cos\theta\ , \tag{11}$$

with maximum instability at $k_c=k_m/\sqrt{3}$.

Each element of the finger profile translates at velocity U in the direction $0x$. Its normal is at an angle θ with $0x$. θ is an increasing function of the curvilinear abscissa s. For each zone of the finger, we may assume that the unstable range of wave vectors is given by Eq. (11). (This would be strictly true only if θ were slowly varying on the scale of the wavelength, which is not realized here.)

In the present case the waves are generated with a finite amplitude near the thread, where $\theta_0\approx 45°$. They can be excited if their wave vector satisfies $k(\theta_0)<k_m(\theta_0)$. In this model all frequencies smaller than

$$f_m(\theta_0)=\frac{U}{2\pi}\frac{\sqrt{12N_{\rm ca}}}{b}\cos\theta_0\sin\theta_0 \tag{12}$$

will generate a wave near the thread. As it is advected away from the thread, the wave affects regions of the profile of increasing values of θ. It undergoes continuous amplification in the region where its wavelength remains in the unstable range given by relation (11). Then it is damped when it reaches the abscissas where θ_1 is such that $f_m(\theta_1)\le f$.

Figures 11(a)–11(c) show the amplification and damping of these waves at three different frequencies. The overall aspect of the envelopes of the waves are qualitatively in agreement with this model. There is strong amplification in the parabolic region of the finger, then damping. The higher the excitation frequency, the shorter the zone on which the wave is amplified. Let us remark that similar experiments carried out in cells of smaller aspect ratio show smaller amplification as the parabolic zone is smaller. To calculate the exact amplitude of the wave, it would be necessary to integrate the growth rate along the profile, starting from the thread.

To get a quantitative estimation of the global amplification we record the effect of modulations at various frequencies on a finger of a given velocity U and measure the wave amplitude at three distances 10ρ, 20ρ, and 40ρ from the tip (Fig. 12). A well-defined maximum is observed at a value f_1, which corresponds to a wavelength $l_1\approx 5.6\rho$ very close to the mean wavelength l_n created by noise of low amplitude. At large distances from the tip, the amplitude of the shorter wavelength drops, due to their damping by surface tension.

In the experimental conditions of Fig. 12, Eq. (10) can give an estimation of the maximum unstable frequency near the thread, $f_m(45°)\approx 7$ Hz. Indeed, no wave is observed at a frequency larger than 8 Hz. The most amplified frequency at the thread would be $f_c(45°)=f_m(45°)/\sqrt{3}\approx 4.1$ Hz, while the wave of larger amplitude corresponds in Fig. 12 to $f_1\approx 4.1$ Hz. The quality of the agreement between a rough theory and the experiment is surprising, but it is worth noting that the orders of magnitude are correct.

The measured amplitudes at low frequencies shown in Fig. 12 are imprecise because the lateral waves correspond in this case to the superposition of harmonics. Even though we apply a sinusoidal modulation to the

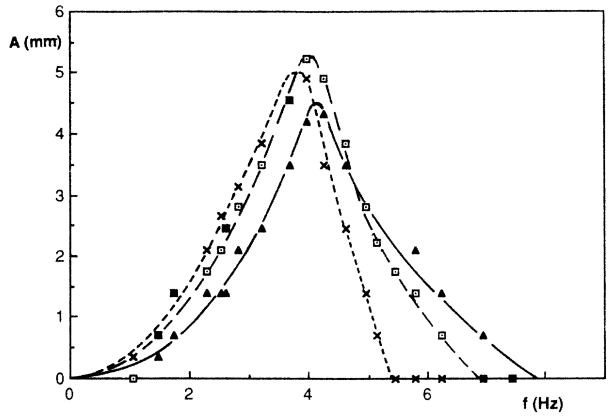

FIG. 12. Amplitude of the forced wave as a function of the excitation frequency (case of a thread and side of the thread), at various distances on the side of the thread. $W=12$ cm, $b=0.1$ cm, $U=5.2$ cm/s, and $\rho=0.23$ cm. ▲ and ——, 10ρ from the tip; □ and — — —, 20ρ from the tip; × and ------, 40ρ from the tip.

pressure, harmonics are present in the resulting modulation of ρ, as the relation between the fingertip radius and the pressure is nonlinear. The wave is strictly sinusoidal when none of its harmonics is in the range of amplified frequencies ($f > f_m/2$). When $f \ll f_m/2$, harmonics can be near f_c, so they are strongly amplified and are visible on the profile of the wave.

IV. CONCLUSION AND DISCUSSION

The main results of the present article can be summarized as follows.

The anomalous fingers form, in the presence of a localized perturbation, a well-defined family of solutions of the Saffman-Taylor problem, stable up to very large velocities.

These fingers are selected by the radius of curvature of their parabolic tip. This radius is scaled on the capillary length.

The observed saturation of ρ at large velocities corresponds to the breakdown of the two dimensionality when ρ becomes of the order of the thickness of the cell.

Using localized disturbance and periodic forcing we have characterized the destabilization of the lateral front of the fingers. We have thus shown experimentally the process of wavelength selection and the stretching of the wave when it is advected along the curved profile.

These results take their full meaning in the following comparison with crystalline dendrites, proving the direct analogy between anomalous fingers and dendrites. Saffman-Taylor fingers grow in the Laplacian pressure field. The front of crystallization which forms the dendrites grows in a temperature field (growth from the melt) or in a concentration field (growth from solution). These fields are governed by a diffusion law. As a result, the viscous fingers grow in an environment defined by the boundary conditions imposed by the cell geometry, while the dendrites grow in an open medium with only a diffusive length scale.

In the first theoretical approaches of each problem, a family of solutions was found in the case of zero surface tension. These were the Saffman-Taylor solutions of Eq. (5) and the Ivantsov parabolas in the case of crystal growth. However, something was missing; in the Saffman-Taylor case no hint was given about which of the solutions was actually selected. In the Ivantsov case only a relation for the product ρU was found.

The next step was the introduction of isotropic surface tension. In the linear Saffman-Taylor experiment, it was theoretically shown that a discrete set of solutions is selected. The lower branch of these solutions is stable and gives rise to the fingers $\lambda=0.5$ which are usually observed. This selection is related to the fact that the linear geometry provides a length scale, W, the width of the channel. In the circular geometry where this length scale does not exist, no stable solution is found. The same lack of external length scale occurs in crystal growth; the solutions found with isotropic surface tension are all unstable by tip splitting. This was actually experimentally observed by Honjo *et al.*[37] They grow crystals between corrugated plates. The resulting noise is strong enough to destroy the effect of anisotropy. The patterns they obtain resemble the viscous fingers in a circular experiment; the fingers are disordered and dominated by tip-splitting processes.

Finally, anisotropic surface tension, or equivalently, localized disturbance of the tip, can be introduced in both problems. It gives rise to anomalous fingers and to crystalline dendrites. We have shown that, in the linear Saffman-Taylor geometry, the scale imposed by the lateral walls becomes secondary and the finger is now determined by its parabolic front and the scale l_0. In both the fingers and the dendrites[31] a continuous family of solutions is observed with a parabolic tip. Their radius of curvature and their velocity are determined by the externally applied constraint (pressure or undercooling) and by anisotropy. They are related to each other by the law

$$\rho^2 U = \text{const.}$$

The destabilization of anomalous fingers, as well as that of dendrites, is characterized by the growth of a lateral instability. The unstable part of a finger corresponds to the parabolic region and its extent is related to the width of the channel. It is only in very wide cells that the destabilization can be compared to that of dendrites. In these cases we have shown that the mean wavelength on the side of the finger is scaled on the radius of curvature at the tip exactly as it is in dendrites. In both cases the instability is due to the selective amplification of noise at the tip.

We wish here to comment further about the characteristic of the growth of the lateral waves, in more general terms, which allow comparison with the growth of other hydrodynamic instabilities. Whenever an instability grows in an infinite medium where Galilean invariance has been broken, Huerre *et al.*[38] have shown that the growth can be described either as a temporal process (absolute instability) or as a spatial one (convective instability). The second case occurs when the advection ve-

locity of the unstable medium is larger than the group velocity of all amplified waves. There is then no feedback process, so that the growth of the instability is spatial and corresponds to the selective amplification of incident noise. Our results obtained with grooves or with a thread show that the growth of the instability in the finger frame of reference is of a convective type. This is why the selection of the growing wavelength is a broadband process due to selective amplification of noise incident at the tip. The same characteristics have been demonstrated in the experiments of Dougherty *et al.*[39] With the fingers, as well as with the dendrites, very large rates of growth of the waves are observed. In the case of dendrites these rates have been calculated numerically by Kessler and Levine[40] and analytically by Langer[41] using a Wentzel-Kramers-Brillouin method.

We have shown that it is possible to force the instability by a time periodic modulation of the constraint. This perturbation is amplified if it is in the correct range of frequency. As its initial amplitude is larger than the natural noise, the external modulation dominates the destabilization of the finger. The lateral side branching then becomes strictly periodic. Our experiment strongly suggests that a similar periodic forcing should also be effective in the case of dendrites. It might then be possible to observe strictly periodic side branching by modulating the undercooling in the adequate frequency range (insofar as the thermic relaxation time of the experiment is not too large).

Finally, it appears that a different regime of destabilization can be observed both in the anomalous fingers and in the dendrites. It is characterized by periodic coherent side branching resulting from a pulsating tip. In the case of fingers it is observed with a bubble at the tip and can be ascribed to the natural forcing of the finger tip by the bubble acting as a local oscillator. In the case of dendrites a similar regime has been observed by Morris *et al.*,[42] Honjo *et al.*,[43] and Rolley *et al.*,[44] all working in concentration diffusive fields. The process responsible for the periodic resonance of the tip of these dendrites is still unknown.

ACKNOWLEDGMENT

We are grateful to H. Thomé for his help during these experiments.

[1]P. G. Saffman and G. I. Taylor, Proc. R. Soc. London, Ser. A **245**, 312 (1958).

[2]P. G. Saffman, J. Fluid Mech. **173**, 73 (1986).

[3]G. M. Homsy, Ann. Rev. Fluid Mech. **19**, 271 (1987).

[4]D. Bensimon, L. P. Kadanoff, S. Liang, B. I. Shraiman, and Chao Tang, Rev. Mod. Phys. **58**, 977 (1986).

[5]R. L. Chuoke, P. Van Meurs, and C. Van der Pol, Trans. Metall. Soc. AIME **216**, 188 (1959).

[6]J. Bataille, Rev. Inst. Fr. Pet. **23**, 1349 (1968).

[7]C. W. Park and G. M. Homsy, Phys. Fluids **28**, 1583 (1986).

[8]The result that $\lambda \rightarrow 0.5$ as $1/B$ grows is best verified in two-dimensional simulations. In real cells, Tabeling *et al.* have shown that the effect of the liquid film left on the glass plates could not be neglected. In particular, the saturation at $\lambda = 0.5$ is not strictly observed and slightly smaller values of λ can be reached [P. Tabeling, G. Zocchi, and A. Libchaber, J. Fluid Mech. **177**, 67 (1987)].

[9]J. W. McLean and P. G. Saffman, J. Fluid Mech. **102**, 455 (1981).

[10]G. Tryggvason and H. Aref, J. Fluid Mech. **136**, 1 (1983); **154**, 287 (1985).

[11]A. J. Degregoria and L. W. Schwartz, J. Fluid Mech. **164**, 383 (1986).

[12]J. M. Vanden-Broeck, Phys. Fluids **26**, 2033 (1983).

[13]R. Combescot, T. Dombre, V. Hakim, Y. Pomeau, and A. Pumir, Phys. Rev. Lett. **58**, 2036 (1986).

[14]B. Shraiman, Phys. Rev. Lett. **56**, 2028 (1986).

[15]D. C. Hong and J. Langer, Phys. Rev. Lett. **56**, 2032 (1986).

[16]D. A. Kessler and H. Levine, Phys. Rev. A **32**, 1930 (1985).

[17]D. Bensimon, Phys. Rev. A **33**, 1302 (1986).

[18]S. Tanveer, Phys. Fluids **30**, 2319 (1987).

[19]Y. Couder, N. Gerard, and M. Rabaud, Phys. Rev. A **34**, 5175 (1986).

[20]This technique had been inspired by a previous observation by Grace and Harrison that the introduction of wires or rods changed the ascending velocity of bubbles in a vertical Hele-Shaw cell [J. R. Grace and D. Harrison, Chem. Eng. Sci. **22**, 1337 (1967)].

[21]D. A. Kessler, J. Koplik, and H. Levine, Phys. Rev. A **34**, 4980 (1986).

[22]A. T. Dorsey and O. Martin (unpublished).

[23]D. C. Hong and J. S. Langer, Phys. Rev. A **36**, 2325 (1987).

[24]G. Zocchi, B. E. Shaw, A. Libchaber, and L. P. Kadanoff, (unpublished).

[25]In the axisymmetric geometry, a larger number of possible disturbances have been investigated. They are all characterized by the fact that they inhibit tip splitting. The finger then exhibits strong side branching, which makes its shape analogous to crystalline dendrites. This effect was first observed by Ben Jacob *et al.* (Ref. 26) in a cell where one of the plates was very deeply engraved with periodic grooves, a technique used also more recently by Horváth *et al.* (Ref. 27). Couder *et al.* (Ref. 28) showed that a similar effect could be obtained by disturbing the tip only with a small bubble. In the case where the viscous fluid is a nematic liquid crystal [Buka *et al.* (Ref. 29)], the flow in front of each finger orients the molecules so that flow-induced anisotropy appears. In a certain range of velocities anomalous fingers are observed.

[26]E. Ben Jacob, R. Godbey, N. D. Goldenfeld, J. Koplik, H. Levine, T. Mueller, and L. M. Sander, Phys. Rev. Lett. **55**, 1315 (1985).

[27]V. Horváth, T. Vicsek, and J. Kertész, Phys. Rev. A **35**, 2553 (1987).

[28]Y. Couder, O. Cardoso, D. Dupuy, P. Tavernier, and W. Thom, Europhys. Lett. **2**, 437 (1986).

[29]A. Buka, J. Kertesz, and T. Vicsek, Nature (London) **323**, 424 (1986).

[30]G. I. Taylor and P. G. Saffman, Q. J. Mech. Appl. Math. **12**, 265 (1959).

[31]C. Huang and M. E. Glicksman, Acta Metall. **29**, 701 (1982).

[32]L. Paterson, Phys. Fluids **28**, 26 (1985).

[33]Ya. B. Zel'dovich, A. G. Istratov, N. I. Kidin, and V. B. Librovich, Combust. Sci. Technol. **24**, 1 (1980).
[34]P. Pelcé, Thèse d'état de l'Université de Provence, 1986; P. Pelcé and P. Clavin, Europhys. Lett. **3**, 907 (1987).
[35]Taking into account an eventual effect of surface tension would produce a lower tangential velocity, so that kinematic stretching would be weaker than $\sqrt{2}$.
[36]B. Caroli, C. Caroli, and B. Roulet, J. Phys. **48**, 1423 (1987).
[37]H. Honjo, S. Ohta, and M. Matsushita, J. Phys. Soc. Jpn. **55**, 2487 (1986).
[38]P. Huerre and P. A. Monkewitz, J. Fluid Mech. **159**, 151 (1985).
[39]A. Dougherty, P. D. Kaplan, and J. P. Gollub (unpublished).
[40]D. A. Kessler and H. Levine, Europhys. Lett. **4**, 215 (1987).
[41]J. S. Langer, Phys. Rev. A **36**, 3350 (1987).
[42]L. R. Morris and W. C. Winegard, J. Cryst. Growth **1**, 245 (1967).
[43]H. Honjo, S. Ohta, and Y. Sawada, Phys. Rev. Lett. **55**, 841 (1985).
[44]E. Rolley, S. Balibar, and F. Gallet, Europhys. Lett. **2**, 247 (1986).

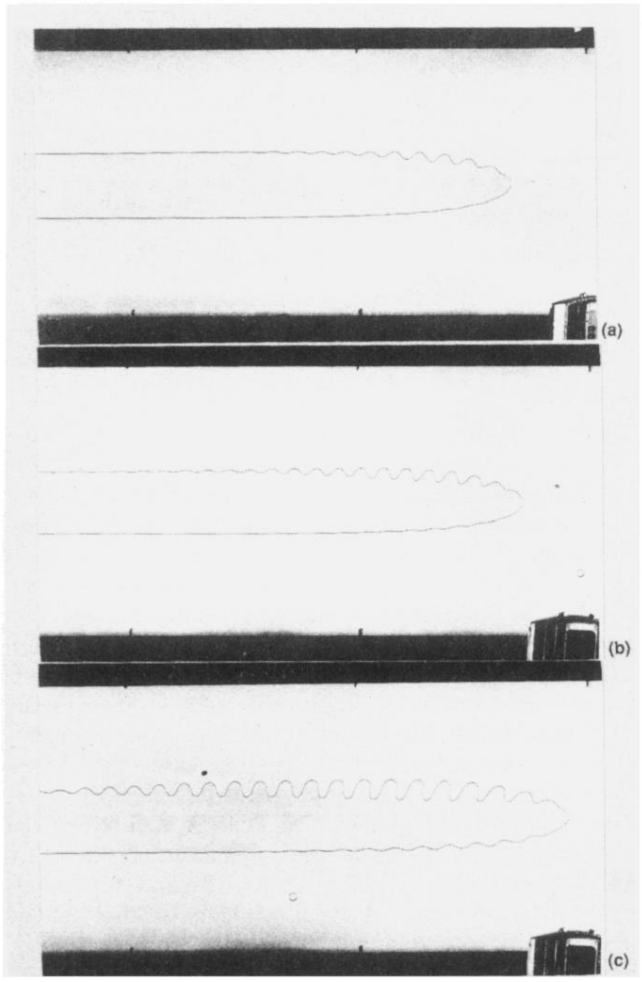

FIG. 11. Aspect of the wave generated on a finger (case of a thread) at different forcing frequencies ($W = 12$ cm, $b = 0.1$ cm). (a) $f \approx f_m$, (b) $f_c < f < f_m$, (c) $f \approx f_c$.

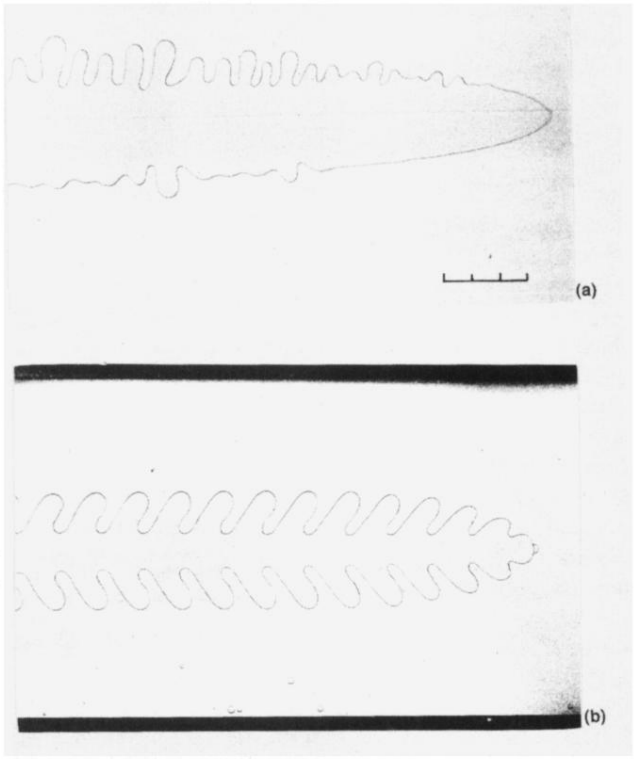

FIG. 6. (a) Spontaneous destabilization of anomalous fingers in a cell of width $W=28$ cm and $b=0.1$ cm disturbed by a thread. As the finger is very narrow ($\lambda=0.18$), only the central region of the cell is shown on this photograph and the lateral walls are far on each side. The scale is in centimeters. (b) A resonant mode obtained with a bubble in a cell $W=12$ cm and $b=0.1$ cm. The outer envelope of this oscillating symmetrical mode corresponds to a solution of Eq. (5) for $\lambda'=0.36$.